THE UNIVERSITY of ADELAIDE

Investigating the role of irinotecan on trabecular long bone in a rat model of breast cancer

A thesis submitted in partial fulfilment of the

HONOURS DEGREE of BACHELOR OF

HEALTH AND MEDICAL SCIENCES In

The Discipline of Anatomy and Pathology

Adelaide Medical School

The University of Adelaide

by Bailey Deverell

November 2020

Abstract

In advanced breast cancer, chemotherapeutic agents are detrimental to bone microarchitecture, increasing fracture risk. Given 90% of individuals treated for breast cancer with chemotherapy survive five-years post-diagnosis, determining effects of chemotherapies on bone is essential. Irinotecan is a chemotherapy drug being trialled for breast cancer treatment, however its effect on bone structure and turnover is yet to be studied. This study aimed to determine irinotecan's effect on trabecular bone in the femur and tibia of a rat model of breast cancer via micro-CT, immunohistochemistry and ELISA analysis.

Female dark agouti rats were subcutaneously inoculated with breast cancer cells and allocated to two groups; vehicle control (n = 8) and irinotecan (175 mg/kg intraperitoneally; n = 8). Five days after treatment, bone microarchitecture was assessed in the femur and tibia via *ex-vivo* micro-CT for; trabecular thickness (Tb.Th.), trabecular number (Tb.N.), trabecular spacing (Tb.S.), bone volume (BV), and percent bone volume (BV/TV%). Femur and tibia sections were then stained with tartrate-resistant acid phosphatase (TRAP) and assessed for osteoclast-like cells and adipocytes. Serum was analysed for c-terminal telopeptide 1 (CTX-1).

Femur and tibia microarchitecture showed no significant difference in Tb.Th., Tb.N. Tb.S. BV or BV/TV% between groups. Irinotecan increased TRAP-positive osteoclast-like cell number on trabecular bone in the tibia compared to vehicle control ($p = 0.033$). CTX-1 ELISA analysis was indeterminate.

Overall, irinotecan increased the number of osteoclasts on trabecular bone however did not cause microarchitectural changes at this time point. Determining when microarchitecture is affected requires further investigation.

Introduction

People treated for cancer with systemic anti-cancer therapies, specifically chemotherapy, are at an increased risk of experiencing adverse effects to their bone health which may eventuate in osteoporosis and higher risk of osteoporotic fracture[1, 2]. As a result, several studies have been conducted on a variety of these chemotherapies to determine the effects on bone post-treatment. A notable example is the chemotherapy drug methotrexate (MTX), which has been researched in animal models of cancer and shown that undesirable effects to bone health may be a result of increased osteoclast (bone resorbing cells) formation and/or activity at trabecular long bone sites[3-5], such as the femur and tibia. Increased osteoclast activity in this region causing a reduction of total bone volume, consequently increases fracture risk[6]. It has also been suggested other chemotherapies, like lapatinib and paclitaxel, which reduce bone volume, can trigger an increase in the number of adipocytes in the trabecular region, known as the "bone-fat switch"[6]. This makes determining the extent at which osteoclasts, adipocytes, and total bone health, are affected by chemotherapies of great importance.

Of the cancers treated with chemotherapy, breast cancer is the most prevalent cancer in women worldwide[7] (not including non-melanoma skin cancers). This prevalence also makes breast cancer the second leading cause of death in Australian women, with an estimated 19,500 cases in 2019 alone[8]. Advancements in the therapies used to treat breast cancer however have enabled 90% of those diagnosed with the disease to survive five-years post diagnosis[9]. It is estimated that 70% of total cancer deaths reveal bone loss at autopsy[10] and 73% of breast cancers metastasise to the bone, which amplifies this effect[11, 12]. As some breast cancers are oestrogen-hormone dependent, they are commonly treated with anti-oestrogen therapies such as selective oestrogen receptor modulators (SERMs)[13]. These treatments aim to significantly deplete oestrogen levels to eradicate breast cancer or prevent recurrence, which results in negative

effects to bone density loss, as bone is also oestrogen dependent[4, 14]. This occurs as a direct result of oestrogens modulatory effect on the osteoclastogenesis pathway[15], which causes increased osteoclast activity and survival periods[16], thus contributing to increased bone resorption.

Oestrogen typically has protective qualities on the bone as it is key in the production of bone forming osteoblasts, and with the involvement of osteoprotegerin (OPG), inhibition of osteoclasts[17]. Chemotherapy treatments cause cytokines, such as Interleukin 6 (IL-6) and Tumour Necrosis Factor-alpha (TNFα), to be increased in both the marrow space and trabecular bone, consequently up-regulating osteoclastogenesis[15]. As bone density is decreased by reductions in oestrogen-hormone, like that seen in post-menopausal women, a greater reduction in oestrogen by chemotherapies can have a severe negative effect on bone health[17]. Current cancer hormone therapies used in breast cancer, such as tamoxifen and aromatase inhibitors, have indicated that treated individuals experience a significant loss of both cortical and trabecular bone[18]. However, some chemotherapies, like MTX, are also oestrogen suppressive which contribute to further reductions in bone mineral density[19]. This provides the opportunity to seek alternative chemotherapy treatments, such as irinotecan, which potentially produce lower toxicities in bone by having greater selectivity to cancer cells.

Camptothecin, and its derivative irinotecan, are recognised chemotherapy drugs which target cancers by conversion into active metabolite SN-38[20, 21]. As SN-38, cell death is triggered by trapping the topoisomerase-1 enzyme (TOP1) on DNA, generating cytotoxic protein-linked DNA breakage[22, 23]. Irinotecan is currently being trialled for use in breast cancer treatment, it has shown to be beneficial in the treatment of numerous other cancers, specifically as colon and rectal cancer[20]. However, Irinotecan has several known side effects, many of which relate

to gut health, including mucositis and diarrhoea, as well as myelosuppression[4, 20]. While these side effects are common for many chemotherapeutic agents, reduced gastrointestinal tract (GIT) health seen in mucositis may have an impact on intestinal flora and calcium absorption [19, 24]. This is of particular importance in the context of bone health due to the high permeability that the GIT possesses[25]. This impact has significant potential to effect bone metabolites as reduced pH in the GIT contributes to higher calcium uptake, thus increasing osteoclast formation[25, 26]. However, little is currently known regarding the effects that irinotecan has on bone health, whether individually or in combination with other treatments, specifically at the trabecular region. Therefore, further study is required to elucidate the effects of irinotecan on bone architecture and remodelling.

Given the known effect that chemotherapy treatments' have on multiple organ systems, including bone, the extent at which this occurs is of particular interest. Specifically, that of diminished bone health, resulting from irinotecan used in breast cancer treatment is yet to be elucidated. This includes the mechanism that suspected bone resorption transpires in the trabecular long bone as a result of irinotecan treatment. It is important to address this in the context of breast cancer such that the efficacy of irinotecan for its treatment can be assessed. This is a result of bone being oestrogen-dependent and reduction in oestrogen, and thus increased osteoclast activity, post-survivorship is highly likely[4]. With increased survivorship, the activity of and presence of osteoclasts in the trabecular long bone following irinotecan administration, is of particular significance. Should this gap in the knowledge be filled, through research of the specific changes that occur in trabecular bone; the opportunity will arise to screen for osteoporosis in treated individuals prior to fractures occurring as targeted interventions can be developed. In doing so, the burden on both the individual's and society's quality of life and economical expenditure can be alleviated.

It was hypothesised that irinotecan used in the treatment of breast cancer will increase osteoclast formation and thus cause a greater extent of trabecular bone loss compared to a vehicle control. To test this hypothesis, the primary aim of this study was to determine the effect of irinotecan, in a rat model of breast cancer, on resorption of the trabecular long bone using the following sub-aims: Investigate bone microarchitecture of femur and tibia using micro-computed tomography (micro-CT). This will include assessment of trabecular thickness (Tb.Th), trabecular number (Tb.N), trabecular spacing (Tb.Sp), trabecular bone volume (BV), and trabecular bone volume and tissue volume fraction (BV/TV%)[27]. Determine local trabecular bone turnover, by assessing the presence of osteoclasts and adipocytes in trabecular femur and tibia through histological assessment of tartrate-resistant acid phosphatase (TRAP) staining. Assess systemic bone turnover by measuring serum levels of C-terminal telopeptide (CTX-1; released by osteoclasts) using ELISA techniques[28].

Methods

Breast Cancer Rat Model

Ethics approval was obtained from the University of Adelaide Animal Ethics Committee (33965) in compliance with the National Health and Research Council (Australia) Code of Practice for Animal Care in Research and Training. Dark agouti rats were housed in a 12 hour light/dark cycle and food and water were provided ad libitum.

Sixteen female dark agouti rats aged eight weeks were randomly allocated to two groups (n = 8 per group): each group was interperitoneally (i.p.) injected with either irinotecan (175 mg/kg)[29] or vehicle control (sorbitol lactic acid buffer, pH 3.4). Breast cancer was inoculated by injection of 4 million breast cancer cells into the subcutaneous flank of the female dark agouti rats. These cells were given approximately five days to form a tumour, measured daily by callipers to determine tumour burden, until it had grown to ~1% body weight. On day one of the treatment schedule, rats received a singular i.p. injection of irinotecan or vehicle control. Five days following chemotherapy injection, rats were humanely culled by cardiac puncture. Left and right femur and tibia as well as serum were collected for subsequent analysis.

Justification of Methods

A past study investigated the role of MTX on osteoclastogenesis in a rat model, which indicated that MTX decreased total bone density through an increase in osteoclast synthesis and bone resorption[5]. This study quantified osteoclasts at the trabecular surface using TRAP staining techniques. A similar study investigated the combined and individual effects of chemotherapeutic agents lapatinib and paclitaxel[6], primarily through micro-CT analysis. It was found that the combination treatment in particular, contributed to significant negative impacts to bone health seen by reduced bone volume[6]. Considering trabecular bone has been shown by

multiple studies to be an accurate indicator of effects of chemotherapy on overall bone health[3-5, 30], it is an apt target region to analyse pathological bone loss. By using these techniques, as well as supplementary experiments and data collection, for the quantification of irinotecan's effect on trabecular long bone in a model of breast cancer, more comprehensive findings should be attained.

Micro-computed tomography analysis

Following collection of femur and tibia, bones were fixed in 10% neutral buffered formalin for 24 hours. Following this, bones were transferred to 1 x PBS for seven days. Bone changes were assessed via images obtained at 9 μm/pixel by micro-CT scanner (SkyScan 1276, Bruker, Kontich, Belgium)[31]. Bones were scanned at a source voltage of 85 kV, current 200 μA, isotropic pixel size of 9 μm with a 1 mm thick aluminium filter, rotation step of 0.2, frame averaging of 2 and a total scan time of approximately 30 minutes. Cross-sectional images of the femur and tibia were reconstructed (N-Recon software, Bruker, Kontich, Belgium) and saved in bitmap format. The reconstructed images were re-aligned in 3D as per in-situ orientation (Dataviewer software, Bruker, Kontich, Belgium).

The region of interest (ROI) was selected, ensuring to include only the metaphyseal region of the trabecular bone in the right femur and right tibia (CT Analyser software, Bruker, Figure 1)[32, 33]. This allowed for the exclusion of the growth plate, which has a naturally higher density of osteoclast and osteoblast turnover[34] . For each femur, 450 cross-sections (corresponding to a length of 4.61 mm) starting from the base of the femoral head distally down the femoral shaft was used for analysis (Figure 1 A-B)[35]. For each tibia, 400 cross-sections (corresponding to a length of 4.10 mm) starting 60 cross-sections distally from the growth plate centre and ending

in the tibial shaft were used for analysis (Figure 1 C-D)[35]. The trabecular region was then selected by tracing serial transverse sections for femur and tibia (Figure 1 B & D) to create the volume of interest (VOI) for trabecular analysis[33].

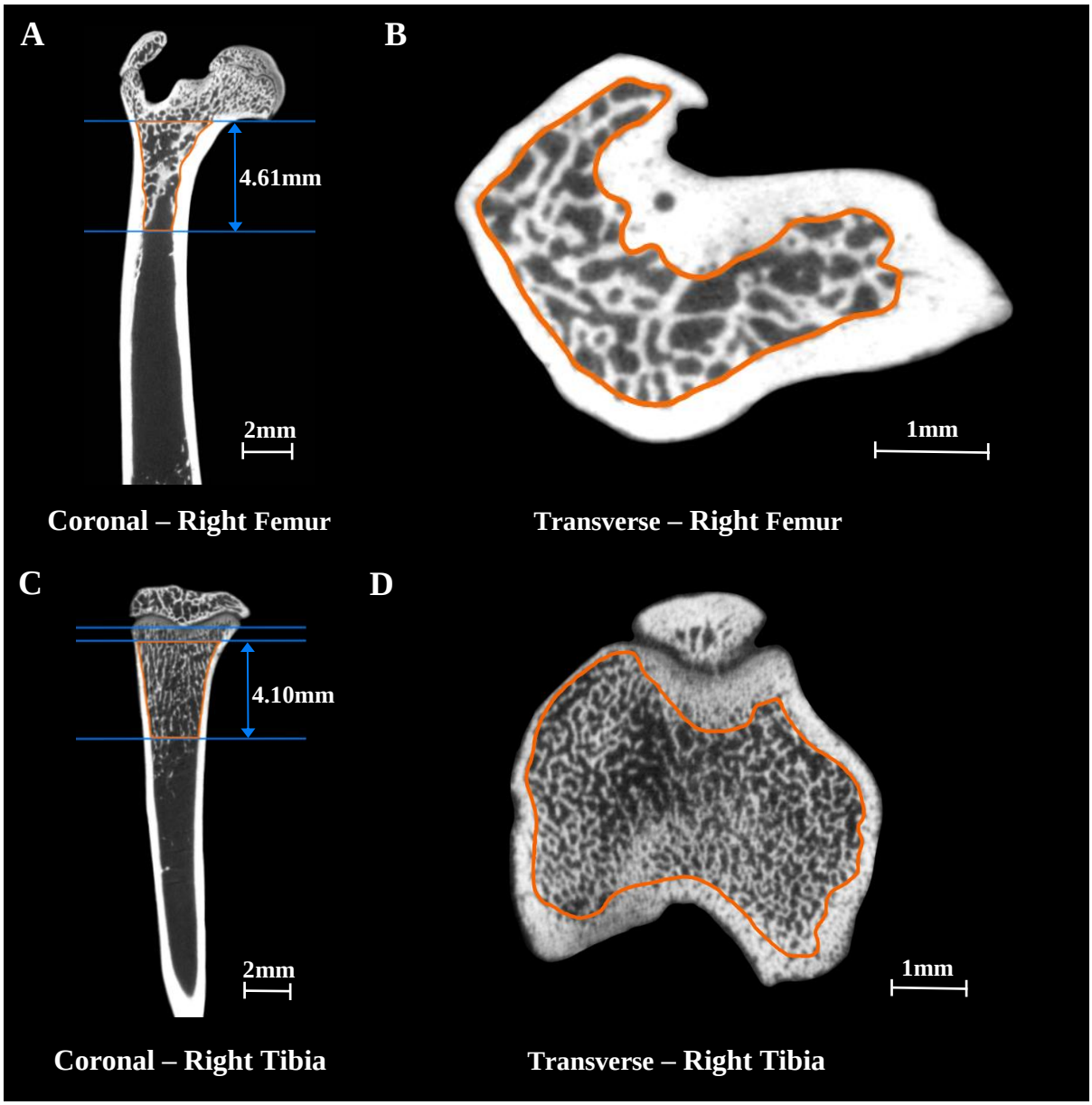

Figure 1. Two-dimensional micro-CT images of proximal right femur (A-B) and proximal right tibia (C-D). Total ROI represented by solid orange line (A-D). Lengths of ROI used for bone analysis are indicated by the blue arrows. Coronal section vertical ROI distance (450 cross sections, corresponding to 4.6 mm; and 400 cross sections, corresponding to 4.1 mm respectively) (A&C). Transverse section trabecular bone selection ROI (B&D).

On the VOI obtained, Tb.Th. (mm), Tb.N. (1/mm), Tb.S. (mm), BV (mm^3), and BV/TV (%) were quantified in 3D using uniform thresholding (CT Analyser software, Bruker)[33]. In the grey-level histogram of the reconstructed cross-section images a minimum threshold level was used for segmentation of bone pixels from non-bone (minimum threshold level 120 to maximum 255), leaving air and any remaining soft tissue as background[36].

Histological analysis

Following micro-CT, all femur and tibia were decalcified in 10% Ethylene diaminetetraacetic acid (EDTA) and embedded in paraffin wax[35]. Serial sections of each bone were cut (5 μm) and stained with TRAP. TRAP staining is an established method of identifying osteoclasts in tissue as osteoclasts and preosteoclasts are TRAP-positive when stained[37, 38]. TRAP staining was performed using the Tatsuo Suda method[39]. Serial sections were dewaxed using histolene/alcohol series steps and rinsed with MilliQ water. The TRAP solution was prepared according to previous validated methods[37, 38]. Each section was subsequently surrounded using a PAP pen, TRAP solution was added onto each section and incubated in a water bath at 37°C for approximately 45 minutes. Tissues were then washed with MilliQ and counterstained with haematoxylin and cover-slipped using Aquamount.

All slides were scanned using NanoZoomer 2.0 at 40x magnification (Hamamatsu Photonics, Japan) and analysed through images produced using NDP.View2 software (Hamamatsu Photonics). During analysis, osteoclasts were defined as multinucleated TRAP-positive cells, determined by red staining. For quantification of these cells, 1-5 1 mm^2 boxes were randomly placed within the region determined by micro-CT analysis (Figure 1) and cells were counted by a blinded observer, through the use of de-identified file names. An average count of multinucleated TRAP-positive cells was then calculated as cells/mm^2.

Adipocytes were also counted, to explore the previously studied "bone-fat switch" seen in chemotherapies such as lapatinib and paclitaxel[6]. This was performed using the same TRAP-stained slides and 1 mm^2 region of interest boxes. Adipocytes were defined as large, vacant cells with a defined edge and an average count (cells/mm^2) was found. Though, some cells showed cellular debris, they were still included as this was likely due to the thickness of slices displaying portions of cells sitting above the adipocytes.

C-Terminal Telopeptide ELISA

C-terminal telopeptide (CTX-1) is an established indicator of bone resorption in systemic rat serum by signifying products of osteoclast activity and collagen breakdown[28]. The collected blood from the rats at cull was spun to produce the serum used for analysis. CTX-1 levels were assessed in the serum collected from rats using a RatLaps CTX-1 ELISA kit (Immunodiagnostics Systems, Nordic) as per the manufacturers instructions[40].

Statistical Analysis

Statistical analysis was performed using GraphPad Prism 8 (GraphPad software). Unpaired t-test was used to determine differences between irinotecan and vehicle control groups effects on trabecular bone for each of the measured parameters. All values shown are mean with SEM and a p value <0.05 was considered statistically significant.

Results

Micro-CT analysis of trabecular bone

The femoral and tibial VOIs produced through micro-CT analysis indicated no trabecular bone differences between irinotecan treated and vehicle control rats at initial viewing of VOIs (Figure 2A & 3A). Statistical analysis of irinotecan treatment displayed no significant changes to trabecular bone microarchitecture for Tb.Th., Tb.N., Tb.S., BV, and BV/TV% compared to the vehicle control in the femur ($p > 0.05$, Figure 2). In the tibial trabecular bone, irinotecan treatment did not significantly differ from the vehicle control in any of the measured bone parameters ($p > 0.05$, Figure 3).

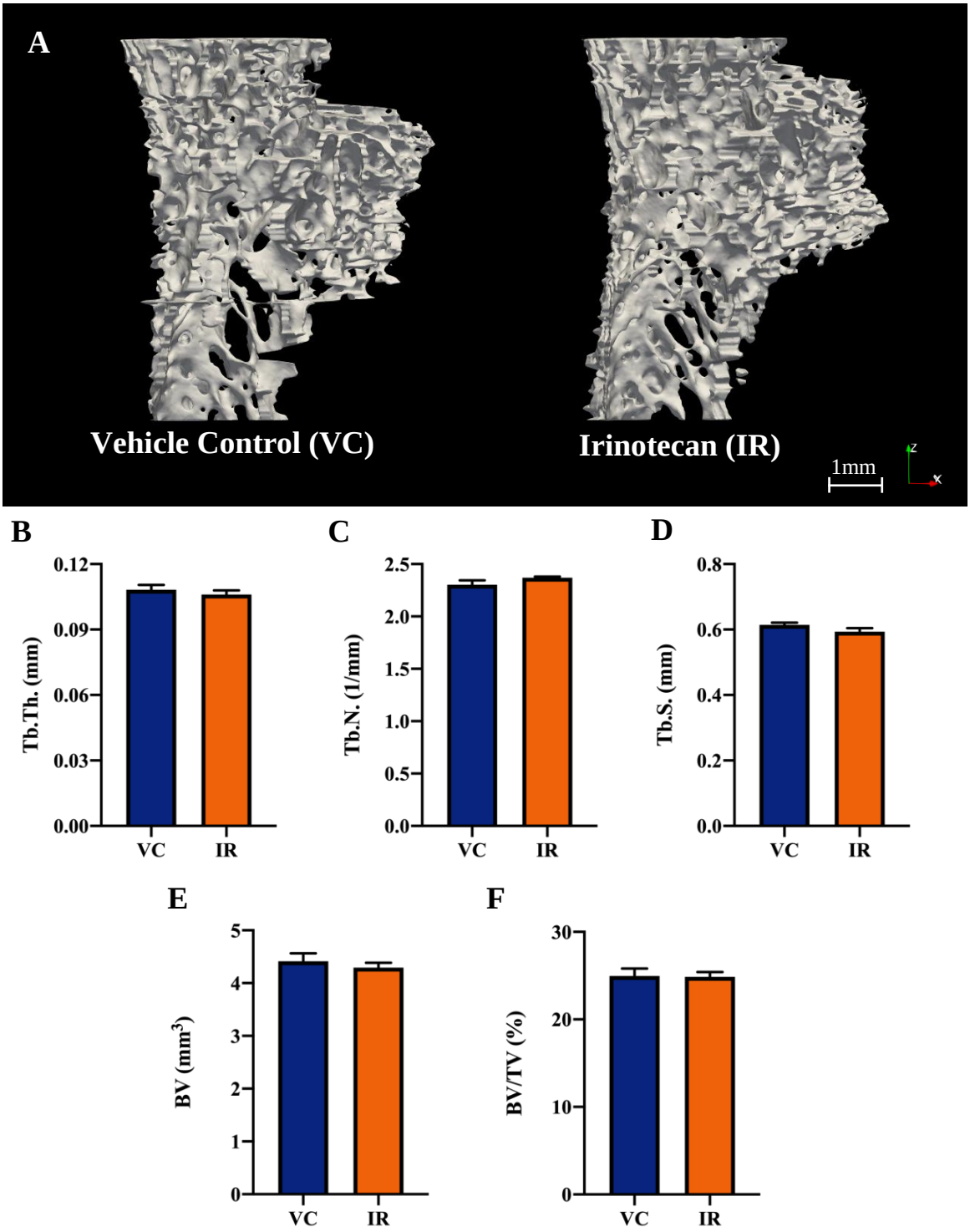

Figure 2. Effect of vehicle control or irinotecan on bone microarchitecture in proximal femoral trabecular region by high resolution micro-CT. Representative three-dimensional micro-CT reconstruction of VOI (A). Analysis of treatment effects in trabecular femur by Tb.Th. (mm), Tb.N. (1/mm), Tb.S. (mm), BV (mm^3), and BV/TV (%) (B-F, respectively). Presented as mean ± SEM (n = 8 per group). Unpaired t-test statistical significance at $P < 0.05$.

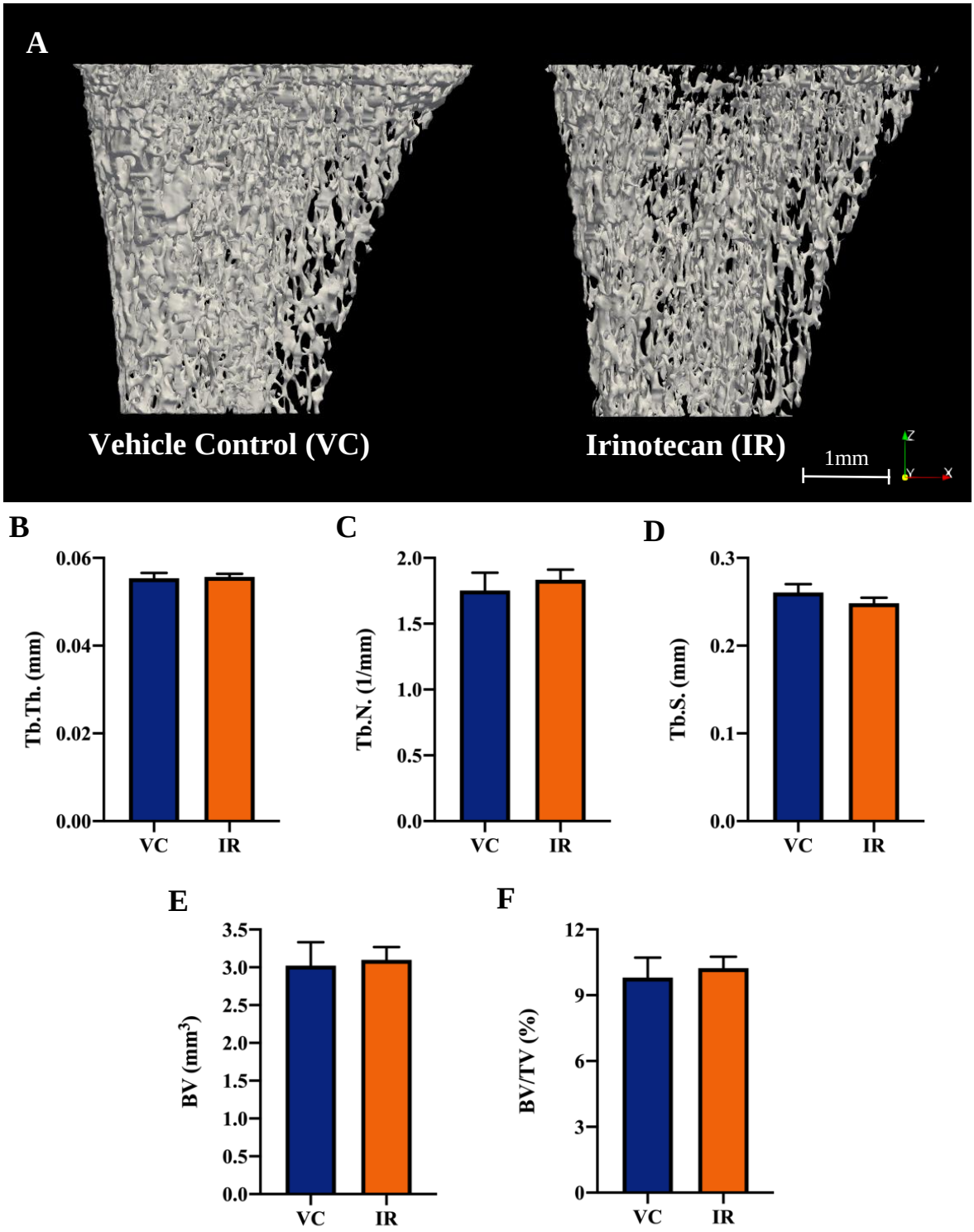

Figure 3. Effect of vehicle control or irinotecan on bone microarchitecture in proximal tibial trabecular region by high resolution micro-CT. Representative three-dimensional micro-CT reconstruction of VOI (A). Analysis of treatment effects in trabecular tibia by Tb.Th. (mm), Tb.N. (1/mm), Tb.S. (mm), BV (mm^3), and BV/TV (%) (B-F, respectively). Presented as mean ± SEM (n = 8 per group). Unpaired t-test statistical significance at $P < 0.05$.

Histological assessment of TRAP staining - Osteoclasts

Histological assessment of TRAP stained femur sections (representative images in Figure 4A) indicated that average multinucleated TRAP-positive cell count in irinotecan treated rats did not significantly differ from vehicle control rats (Figure 4B). In the tibia, irinotecan treatment significantly increased the average number of TRAP-positive multinucleated cells on the bone in the trabecular region of interest (69.46 ± 6.31 cells) compared to the vehicle control (51.51 ± 4.17 cells; *p = 0.033, Figure 5B).

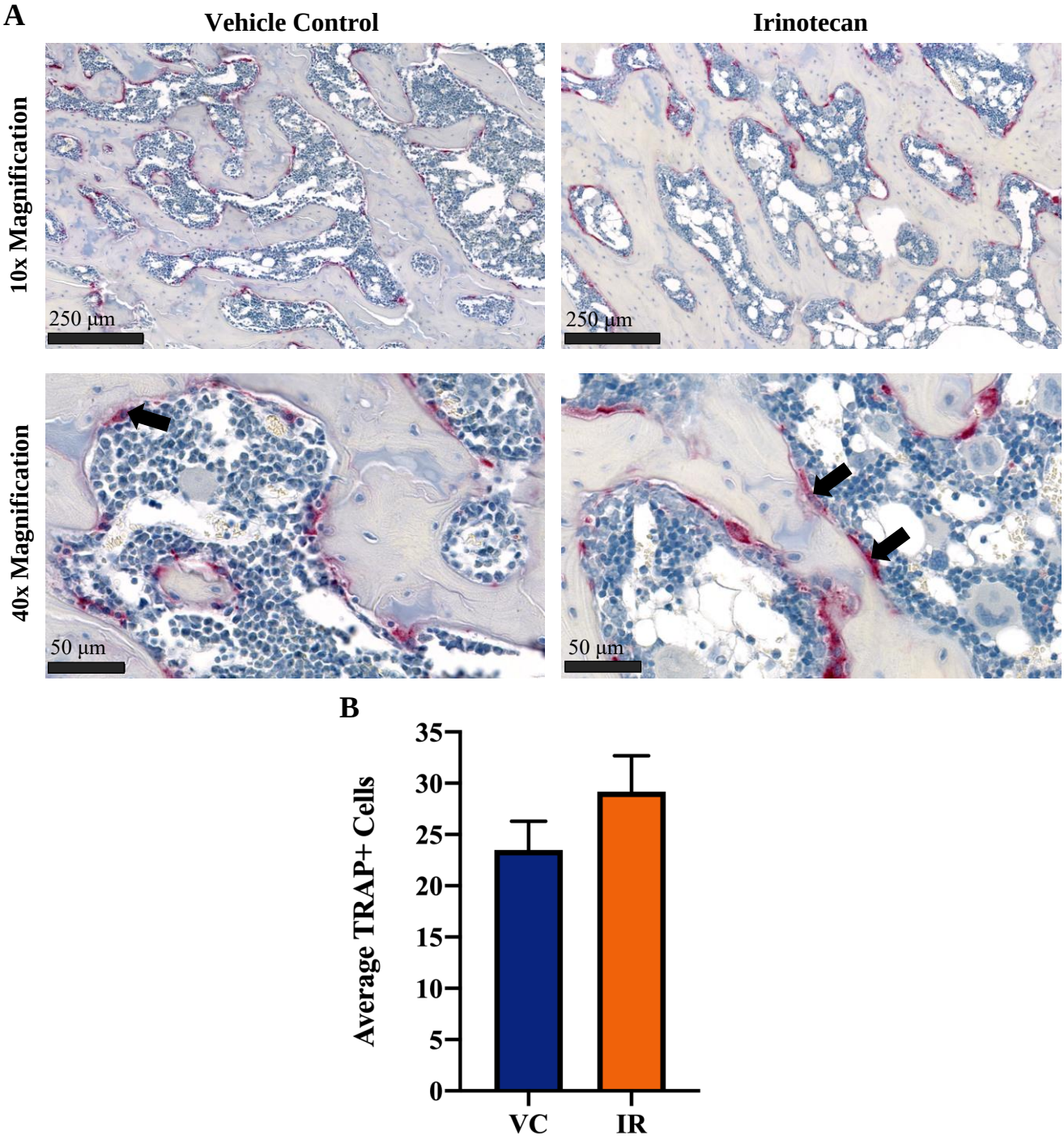

Figure 4. Assessment of osteoclasts in proximal femur trabecular bone. Representative images of femur sections stained with TRAP (indicated by red colouration) with haematoxylin counterstaining, 10x and 40x magnification (A). Arrows indicate some multinucleated TRAP-positive cells. Average TRAP-positive multinucleated cells per mm^2 on the bone surface of irinotecan and vehicle control groups (B). Presented as mean ± SEM (n = 8 per group). Unpaired t-test statistical significance at $P < 0.05$.

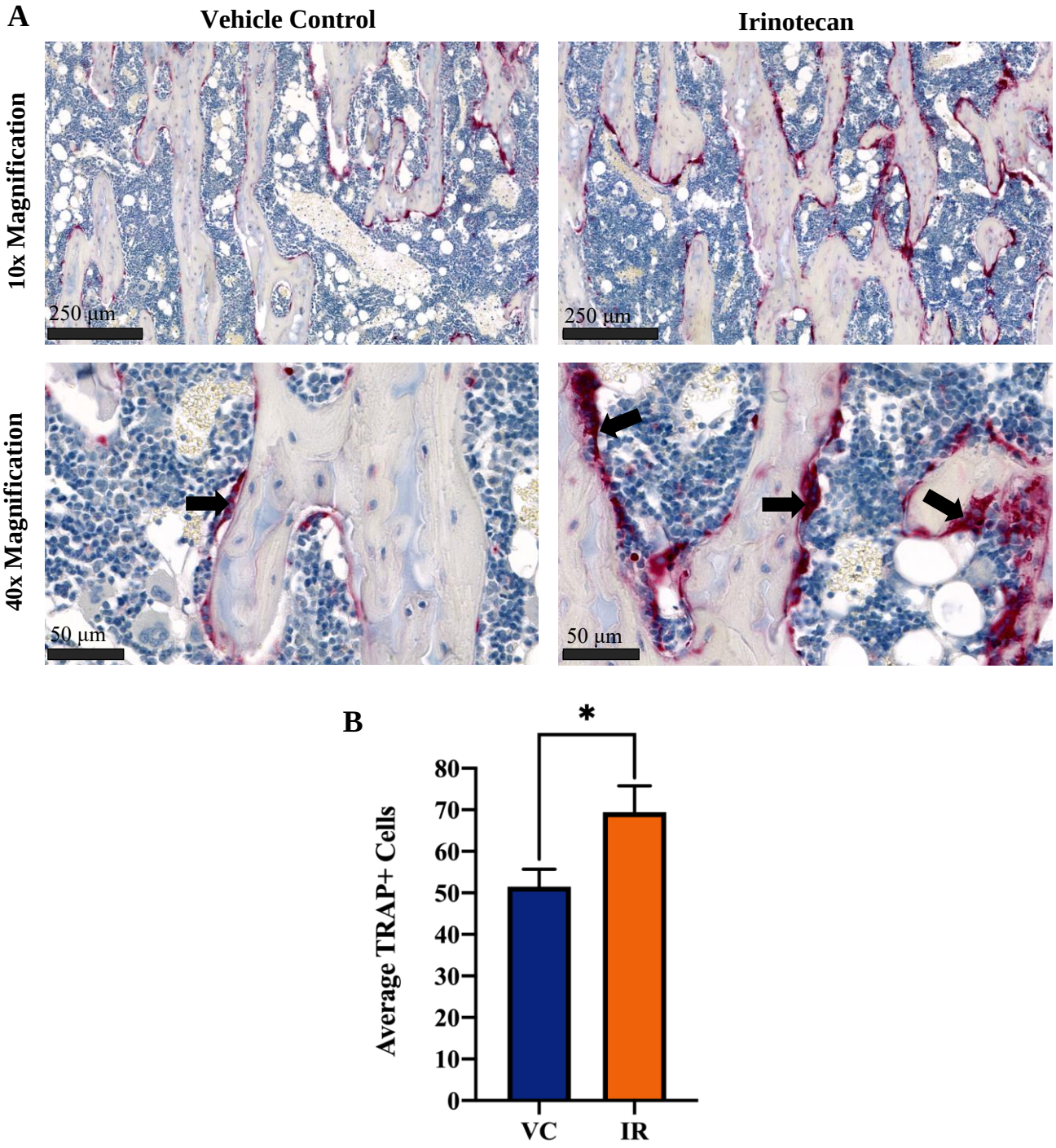

Figure 5. Assessment of osteoclasts in proximal tibia trabecular bone. Representative images of tibia sections stained with TRAP (indicated by red colouration) with haematoxylin counterstaining, 10x and 40x magnification (A). Arrows indicate some multinucleated TRAP-positive cells. Average TRAP-positive multinucleated cells per mm^2 on the bone surface of irinotecan and vehicle control groups (B). Presented as mean ± SEM (n = 8 per group). Unpaired t-test statistical significance at $P < 0.05$.

Histological assessment of TRAP staining - Adipocytes

Adipocyte density in the trabecular region tissue of the femur and tibia are represented in Figures 6A and 7A. In in the femur of the irinotecan treated rats, there was no significant difference in the number of adipocytes per mm^2 in the trabecular tissue region (168.9 ± 30.09 cells) compared to the vehicle control (129.4 ± 16.33 cells) ($p > 0.05$, Figure 6B). In the tibia, there was an no significant difference in the number of adipocytes per mm^2 in the trabecular tissue region of irinotecan treated rats (89.51.9 ± 19.85 cells) compared to the vehicle control (81.53 ± 9.84 cells) ($p > 0.05$, Figure 7B).

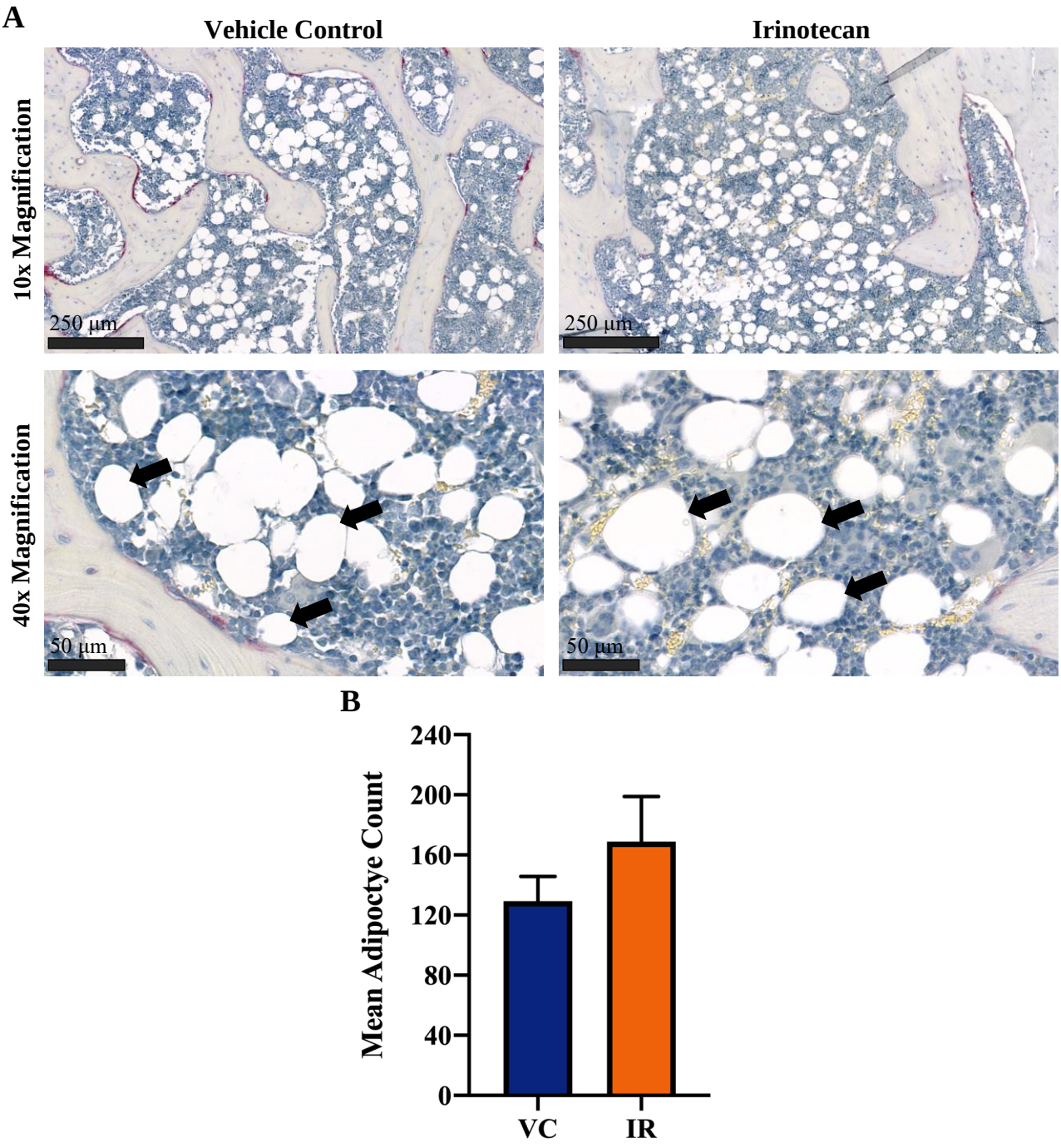

Figure 6. Assessment of adipocyte density in proximal femur trabecular bone. Representative images of femur sections stained with TRAP with haematoxylin counterstaining, 10x and 40x magnification (A). Arrows indicate some adipocytes. Mean adipocytes per mm^2 in region of interested tissue for irinotecan and vehicle control groups (B). Presented as mean ± SEM (n = 8 per group). Unpaired t-test statistical significance at $P < 0.05$.

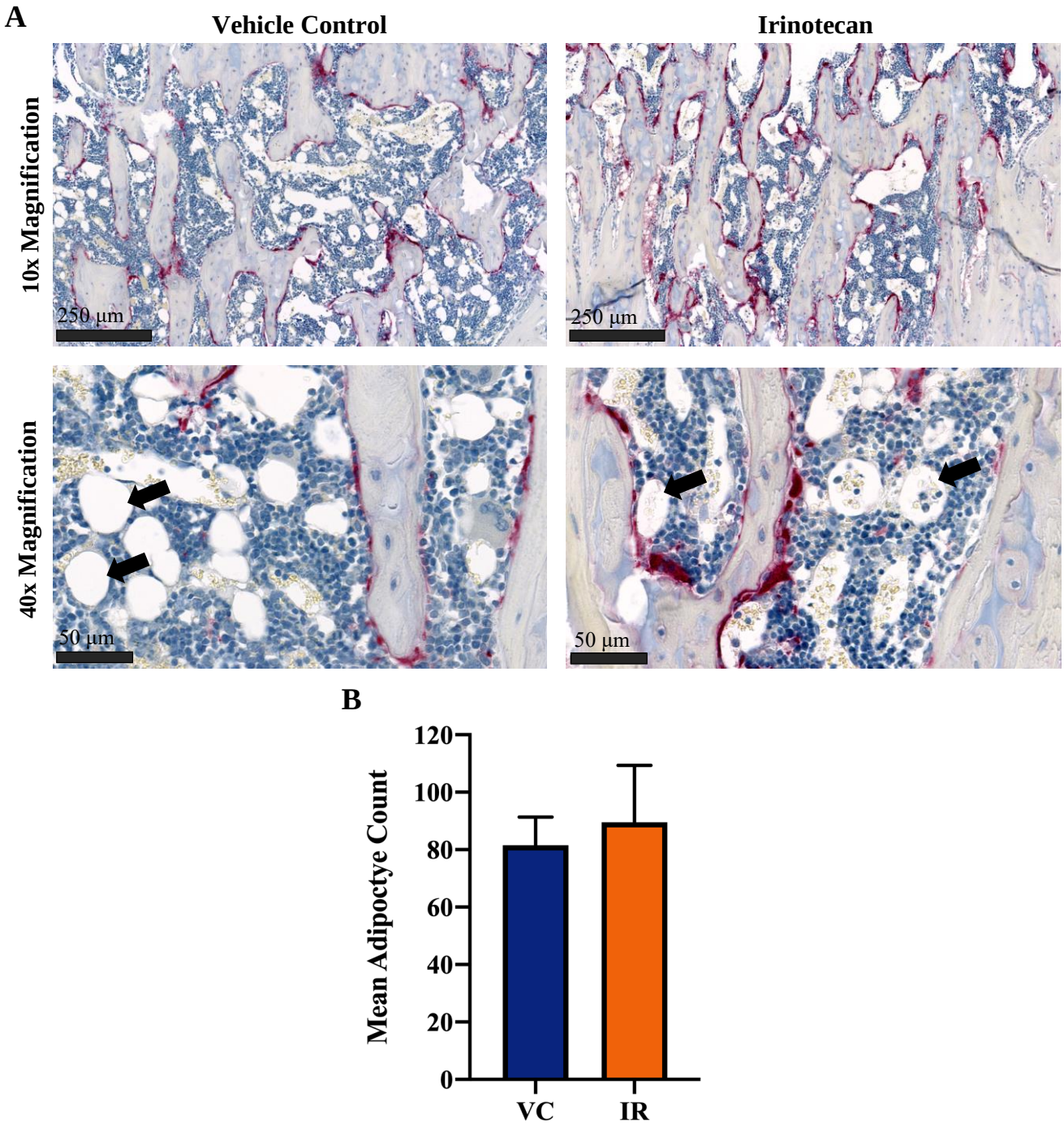

Figure 7. Assessment of adipocyte density in proximal tibia trabecular bone. Representative images of tibia sections stained with TRAP with haematoxylin counterstaining, 10x and 40x magnification (A). Arrows indicate some adipocytes. Mean adipocytes per mm^2 in region of interested tissue for irinotecan and vehicle control groups (B). Presented as mean ± SEM (n = 8 per group). Unpaired t-test statistical significance at $P < 0.05$.

CTX-1 ELISA analysis of serum

C-terminal telopeptide (CTX-1) levels were assessed in the serum collected from both irinotecan and vehicle control treated rats as a systemic marker of bone resorption. CTX-1 levels as assessed by ELISA were indeterminate as they were below a level of detection (data not shown).

Discussion

This study was the first to investigate the relationship between irinotecan and osteoclasts contributing to trabecular bone resorption of the proximal femur and tibia. This was done via macroscopic assessment of tissue microarchitecture, TRAP staining techniques for local analysis of osteoclast-like cell presence and bone adiposity, and serum analysis of CTX-1 bone resorption products. The results suggest that trabecular bone resorption is increased by irinotecan treatment, though a longer model is likely required to appreciate this at a macroscopic level.

Micro-CT assessment of the femur and tibia in Tb.Th., Tb.N., Tb.S., BV, and BV/TV does not reflect the hypothesis which suggested that irinotecan would cause a notable reduction in trabecular bone density by action of increased osteoclast activity. Rather, each of these parameters displayed no significant difference between the irinotecan and vehicle control groups. In accordance with prior literature investigating chemotherapy drugs such as MTX, an increase in trabecular resorption was expected[4, 5]. However, this result may not have been present in this study as a direct result of only using the one cull time point, at five days post administration of irinotecan. This singular cull time was initially implemented based on previous irinotecan studies based on gastrointestinal toxicity, which used five days as the maximum treatment time[41, 42], and may not have provided enough time to appreciate changes in bone degradation assessed at a macroscopic level. Previous studies investigating the effects of chemotherapy on bone have used multiple cull timepoints ranging up to 14 days post treatment[4].

It was expected that osteoclastogenesis would have been increased by day five post-irinotecan treatment due to the role of nuclear factor-κB (NFκB), TNFα and cytokine IL-6 in this process.

Previous studies have indicated that levels of these cytokines are increased in the GIT at as little as two hours post irinotecan administration[20]. This suggests that an increase in osteoclast-like cells would have been evident in the TRAP assessment at the five day timepoint. Following TRAP staining, the average number of TRAP-positive multinucleated cells was only significantly increased by irinotecan compared to the vehicle control in the tibia ($p = 0.033$). Unexpectedly, this was not consistent in the femur with the data indicating no significant differences to osteoclast presence compared to the vehicle control. Significance in the tibial trabecular bone only, may indicate that the tibia possesses a higher susceptibility to developing osteoporosis as a result of irinotecan treatment, or at least doing so at a faster rate, than the femur, though this would need further investigation to determine whether this is accurate.

As an increase in osteoclasts can be seen in the tibia, this could indicate the beginning of the trabecular bone resorption process in this region. The existing correlation of increased osteoclast activation on the trabecular bone surface and its subsequent resorption at a macroscopic level, indicate that there had not been sufficient time for this resorption to occur prior to the cull point. Thus, it is likely that at a later time point, trabecular bone loss could be seen in the microarchitecture through micro-CT. This would indicate that there may be a potential window of time for intervention and screening between initial treatment and damage to the bone itself taking place. This could signify that there is a delayed onset of morphological trabecular bone resorption by osteoclasts, shortly after osteoclast recruitment.

The potential window of time between osteoclast recruitment and trabecular bone resorption may provide an opportunity to screen individuals treated with irinotecan. This may include the use of bisphosphonates which inhibit osteoclastic bone resorption by targeting osteoclast precursors[43]. Bisphophonates are already established as a standard treatment for bone

resorption seen in Paget's disease and osteoporosis[44]. Because of this, the use of bisphosphonates is recognised for reduction in fracture risk, though some adverse effects to the gastroesophageal region, such as increased irritation, have been discovered[45]. More importantly, it has been suggested that the bone formed during bisphosphonate may be of reduced quality, leading to higher susceptibility to micro-cracks and consequently fracture should the drug be used long-term[45-47]. This would mean that should patients be prescribed with bisphosphonates following irinotecan, they would need to be closely monitored to ensure that use is short-term and adequate calcium and vitamin D intake is met, to counteract reduced bone quality[45].

A delayed onset of bone resorption may also explain why there is no significant changes to the adipocyte density between irinotecan and vehicle control groups. The noted reciprocal changes in the "bone-fat switch" following chemotherapies such as lapatinib and paclitaxel[6], and MTX[3] have been attributed to the common precursor of osteoblasts and adipocytes. However, as bone has not yet been significantly diminished by action of osteoclasts in irinotecan treated rats, the "switch" has not yet occurred. Although this same research into paclitaxel and lapatinib, notifies that further studies are required to understand this process.

The CTX-1 ELISA assay was indeterminate in assessing the collected serum. As a competitive assay it was expected that expression of CTX-1 would be indicated by a decreasing standard curve. However, upon analysis the curve produced by the known standards was extremely shallow and there was both little to no detection of CTX-1 presence and differentiation between treatment groups. This indicated that the assay was unsuccessful in producing viable data for further analysis.

Several pathways for future studies exist for research into the irinotecan's effect on trabecular bone in the context of breast cancer. Particularly, a greater range of cull-time points would provide the opportunity to more accurately determine whether this treatment will eventuate in diminished microarchitecture at trabecular bone sites. Should this be as expected a more accurate window of time for screening and intervention could also be established. Further research into the effects of irinotecan on bone could also be aided by the implementation of a healthy rat group, which does not experience tumour inoculation, to ensure that the effects seen are primarily a result of the chemotherapy itself. Furthermore, investigating the effects of irinotecan on bone formation may also be desirable to determine the chemotherapy's effect on bone formation, as well as resorption. Finally, determining the mechanism of irinotecan's action could be investigated through gaining a better understanding of cytokine involvement in osteoclast resorption such as NFκB, TNFα, and IL-6.

In conclusion, this is the first study to investigate the effects of chemotherapeutic drug irinotecan on trabecular long bone in the context of breast cancer. It was found that irinotecan treatment significantly increased the density of multinucleated osteoclasts on the trabecular bone surface of the tibia. However, this had not yet taken effect on the trabecular microarchitecture of this region. Thus, a potential window for screening and treatment may exist shortly after irinotecan administration to counteract bone resorption in patients with higher susceptibility to bone loss and fracture. Further investigation is required to determine where this intervention window lies, as well as to elucidate the mechanism of action by which irinotecan effects osteoclastogenesis.

Acknowledgements

I would like to acknowledge my supervisory team A/Prof Tania Crotti, A/Prof Joanne Bowen and Dr Bonnie Williams and other members of both the Bone and Joint laboratory and Cancer Treatment and Toxicities Group. Particularly, Eleni Tsangari and Bonnie Williams for their invaluable help in the experimental processes of this study. I would also like to acknowledge the help of Dr Emma Bateman, who ran the rat model, and Adelaide Microscopy staff members, Ruth Williams and Agatha Labrinidis, for their technical assistance.

References

1. Guise TA (2006). Bone loss and fracture risk associated with cancer therapy. *Oncologist* **11**, 1121-31.
2. Oh YL, Yoon MS, Suh DS, Kim A, Kim MJ, Lee JY, Song YJ, Ji YI, Kim KH & Chun S (2015). Changes in bone density after cancer treatment in patients with cervical and endometrial cancer. *J Cancer* **6**, 82-9.
3. Georgiou KR, Scherer MA, Fan CM, Cool JC, King TJ, Foster BK & Xian CJ (2012). Methotrexate chemotherapy reduces osteogenesis but increases adipogenic potential in the bone marrow. *J Cell Physiol* **227**, 909-18.
4. Georgiou KR, King TJ, Scherer MA, Zhou H, Foster BK & Xian CJ (2012). Attenuated Wnt/beta-catenin signalling mediates methotrexate chemotherapy-induced bone loss and marrow adiposity in rats. *Bone* **50**, 1223-33.
5. King TJ, Georgiou KR, Cool JC, Scherer MA, Ang ES, Foster BK, Xu J & Xian CJ (2012). Methotrexate chemotherapy promotes osteoclast formation in the long bone of rats via increased pro-inflammatory cytokines and enhanced NF-kappaB activation. *Am J Pathol* **181**, 121-9.
6. Lee AMC, Bowen JM, Su YW, Plews E, Chung R, Keefe DMK & Xian CJ (2019). Individual or combination treatments with lapatinib and paclitaxel cause potential bone loss and bone marrow adiposity in rats. *J Cell Biochem* **120**, 4180-4191.
7. Rojas K & Stuckey A (2016). Breast Cancer Epidemiology and Risk Factors. *Clin Obstet Gynecol* **59**, 651-672.
8. Australian Institute of H & Welfare (2018). Cancer in Australia: Actual incidence data from 1982 to 2013 and mortality data from 1982 to 2014 with projections to 2017. *Asia Pac J Clin Oncol* **14**, 5-15.
9. Youlden DR, Baade PD, Walker R, Pyke CM, Roder DM & Aitken JF (2019). Breast Cancer Incidence and Survival Among Young Females in Queensland, Australia. *J Adolesc Young Adult Oncol* **9**, 402-409

10. Wissing MD (2015). Chemotherapy- and irradiation-induced bone loss in adults with solid tumors. *Curr Osteoporos Rep* **13**, 140-5.

11. Welch DR, Harms JF, Mastro AM, Gay CV & Donahue HJ (2003). Breast cancer metastasis to bone: evolving models and research challenges. *J Musculoskelet Neuronal Interact* **3**, 30-8.

12. Sturgeon KM, Mathis KM, Rogers CJ, Schmitz KH & Waning DL (2019). Cancer- and Chemotherapy-Induced Musculoskeletal Degradation. *JBMR Plus* **3**, e10187.

13. An KC (2016). Selective Estrogen Receptor Modulators. *Asian Spine J* **10**, 787-91.

14. Riggs BL (2000). The mechanisms of estrogen regulation of bone resorption. *J Clin Invest* **106**, 1203-4.

15. Manolagas SC (2000). Birth and death of bone cells: basic regulatory mechanisms and implications for the pathogenesis and treatment of osteoporosis. *Endocr Rev* **21**, 115-37.

16. Eastell R (2005). Role of oestrogen in the regulation of bone turnover at the menarche. *J Endocrinol* **185**, 223-34.

17. Cauley JA (2015). Estrogen and bone health in men and women. *Steroids* **99**, 11-5.

18. Lee SJ, Kim KM, Brown JK, Brett A, Roh YH, Kang DR, Park BW & Rhee Y (2015). Negative Impact of Aromatase Inhibitors on Proximal Femoral Bone Mass and Geometry in Postmenopausal Women with Breast Cancer. *Calcif Tissue Int* **97**, 551-9.

19. Reda H. ElMazoudy HMAe, Ahmed E. Abdelkareem (2014). Developmental Toxicity of Oral Administered Low- and High-Dose of Folate Antagonist, Methotrexate in Female CD-1 Mice. *Int. J. Sci. Res.* **3**, 1791 - 1799.

20. Mayo BJ, Stringer AM, Bowen JM, Bateman EH & Keefe DM (2017). Irinotecan-induced mucositis: the interactions and potential role of GLP-2 analogues. *Cancer Chemother Pharmacol* **79**, 233-249.

21. Fakiha K, Coller JK, Logan RM, Gibson RJ & Bowen JM (2019). Amitriptyline prevents CPT-11-induced early-onset diarrhea and colonic apoptosis without reducing overall gastrointestinal damage in a rat model of mucositis. *Support Care Cancer* **27**, 2313-2320.

22. Bao X, Wu J, Kim S, LoRusso P & Li J (2019). Pharmacometabolomics Reveals Irinotecan Mechanism of Action in Cancer Patients. *J Clin Pharmacol* **59**, 20-34.

23. Kumler I, Brunner N, Stenvang J, Balslev E & Nielsen DL (2013). A systematic review on topoisomerase 1 inhibition in the treatment of metastatic breast cancer. *Breast Cancer Res Treat* **138**, 347-58.

24. Chen YC, Greenbaum J, Shen H & Deng HW (2017). Association Between Gut Microbiota and Bone Health: Potential Mechanisms and Prospective. *J Clin Endocrinol Metab* **102**, 3635-3646.

25. Zhang J, Lu Y, Wang Y, Ren X & Han J (2018). The impact of the intestinal microbiome on bone health. *Intractable Rare Dis Res* **7**, 148-155.

26. Xu X, Jia X, Mo L, Liu C, Zheng L, Yuan Q & Zhou X (2017). Intestinal microbiota: a potential target for the treatment of postmenopausal osteoporosis. *Bone Res* **5**, 17046.

27. King TJ, Shandala T, Lee AM, Foster BK, Chen KM, Howe PR & Xian CJ (2015). Potential Effects of Phytoestrogen Genistein in Modulating Acute Methotrexate Chemotherapy-Induced Osteoclastogenesis and Bone Damage in Rats. *Int J Mol Sci* **16**, 18293-311.

28. Williams B, Tsangari E, Stansborough R, Marino V, Cantley M, Dharmapatni A, Gibson R, Perilli E & Crotti T (2017). Mixed effects of caffeic acid phenethyl ester (CAPE) on joint inflammation, bone loss and gastrointestinal inflammation in a murine model of collagen antibody-induced arthritis. *Inflammopharmacology* **25**, 55-68.

29. Gibson RJ, Bowen JM, Alvarez E, Finnie J & Keefe DM (2007). Establishment of a single-dose irinotecan model of gastrointestinal mucositis. *Chemotherapy* **53**, 360-9.

30. Xian CJ, Cool JC, Scherer MA, Macsai CE, Fan C, Covino M & Foster BK (2007). Cellular mechanisms for methotrexate chemotherapy-induced bone growth defects. *Bone* **41**, 842-50.

31. Perilli E, Baruffaldi F, Visentin M, Bordini B, Traina F, Cappello A & Viceconti M (2007). MicroCT examination of human bone specimens: effects of polymethylmethacrylate embedding on structural parameters. *J Microsc* **225**, 192-200.

32. Liu H, Li W, Liu YS & Zhou YS (2016). Bone micro-architectural analysis of mandible and tibia in ovariectomised rats: A quantitative structural comparison between undecalcified histological sections and micro-CT. *Bone Joint Res* **5**, 253-62.

33. Mohan G, Perilli E, Kuliwaba JS, Humphries JM, Parkinson IH & Fazzalari NL (2011). Application of in vivo micro-computed tomography in the temporal characterisation of subchondral bone architecture in a rat model of low-dose monosodium iodoacetate-induced osteoarthritis. *Arthritis Res Ther* **13**, R210.

34. Moreira CA, Dempster DW & Baron R (2000). Anatomy and Ultrastructure of Bone - Histogenesis, Growth and Remodeling. In *Endotext*, edn, ed. Feingold KR, Anawalt B, Boyce A, Chrousos G, de Herder WW, Dungan K, Grossman A, Hershman JM, Hofland HJ, Kaltsas G, Koch C, Kopp P, Korbonits M, McLachlan R, Morley JE, New M, Purnell J, Singer F, Stratakis CA, Trence DL & Wilson DP. South Dartmouth (MA).

35. Williams B, Lees F, Tsangari H, Hutchinson MR, Perilli E & Crotti TN (2020). Assessing the Effects of Parthenolide on Inflammation, Bone Loss, and Glial Cells within a Collagen Antibody-Induced Arthritis Mouse Model. *Mediators Inflamm* **2020**, 6245798.

36. Perilli E, Cantley M, Marino V, Crotti TN, Smith MD, Haynes DR & Dharmapatni AA (2015). Quantifying not only bone loss, but also soft tissue swelling, in a murine inflammatory arthritis model using micro-computed tomography. *Scand J Immunol* **81**, 142-50.

37. Burstone MS (1959). Histochemical demonstration of acid phosphatase activity in osteoclasts. *J Histochem Cytochem* **7**, 39-41.

38. Gravallese EM, Harada Y, Wang JT, Gorn AH, Thornhill TS & Goldring SR (1998). Identification of cell types responsible for bone resorption in rheumatoid arthritis and juvenile rheumatoid arthritis. *Am J Pathol* **152**, 943-51.

39. Yasuda H, Shima N, Nakagawa N, Yamaguchi K, Kinosaki M, Mochizuki S, Tomoyasu A, Yano K, Goto M, Murakami A, Tsuda E, Morinaga T, Higashio K, Udagawa N, Takahashi N & Suda T (1998). Osteoclast differentiation factor is a ligand for osteoprotegerin/osteoclastogenesis-inhibitory factor and is identical to TRANCE/RANKL. *Proc Natl Acad Sci U S A* **95**, 3597-602.

40. Dharmapatni AA, Cantley MD, Marino V, Perilli E, Crotti TN, Smith MD & Haynes DR (2015). The X-Linked Inhibitor of Apoptosis Protein Inhibitor Embelin Suppresses

Inflammation and Bone Erosion in Collagen Antibody Induced Arthritis Mice. *Mediators Inflamm* **2015**, 564042.

41. Wardill HR, Bowen JM, Al-Dasooqi N, Sultani M, Bateman E, Stansborough R, Shirren J & Gibson RJ (2014). Irinotecan disrupts tight junction proteins within the gut : implications for chemotherapy-induced gut toxicity. *Cancer Biol Ther* **15**, 236-44.

42. Al-Dasooqi N, Bowen J, Bennett C, Finnie J, Keefe D & Gibson R (2017). Cell adhesion molecules are altered during irinotecan-induced mucositis: a qualitative histopathological study. *Support Care Cancer* **25**, 391-398.

43. O'Carrigan B, Wong MH, Willson ML, Stockler MR, Pavlakis N & Goodwin A (2017). Bisphosphonates and other bone agents for breast cancer. *Cochrane Database Syst Rev* **10**, CD003474.

44. Russell RG & Rogers MJ (1999). Bisphosphonates: from the laboratory to the clinic and back again. *Bone* **25**, 97-106.

45. Kennel KA & Drake MT (2009). Adverse effects of bisphosphonates: implications for osteoporosis management. *Mayo Clin Proc* **84**, 632-7; quiz 638.

46. Jin A, Cobb J, Hansen U, Bhattacharya R, Reinhard C, Vo N, Atwood R, Li J, Karunaratne A, Wiles C & Abel R (2017). The effect of long-term bisphosphonate therapy on trabecular bone strength and microcrack density. *Bone Joint Res* **6**, 602-609.

47. Ma S, Goh EL, Jin A, Bhattacharya R, Boughton OR, Patel B, Karunaratne A, Vo NT, Atwood R, Cobb JP, Hansen U & Abel RL (2017). Long-term effects of bisphosphonate therapy: perforations, microcracks and mechanical properties. *Sci Rep* **7**, 43399.